

Static and dynamic thermo mechanical characterization of a bio-compatible shape-memory polymer

Pauline Butaud^{1*}, Anne Maynadier², Nicolas Brault, Vincent Placet¹, Morvan Ouisse¹, Emmanuel Foltête¹, Cécile Rogueda-Berriet¹

¹ FEMTO-ST Applied Mechanics Department, Besançon, FRANCE

² LaMCoS Laboratoire de Mécanique des Contacts et des Structures, Lyon, FRANCE

Abstract

Shape memory polymers encounter a growing interest over the past ten years particularly because their eventual bio-compatibility leads to many bio-medical applications. They also present many benefits for the design of micro-adaptive systems for deployment or controlled damping materials. Indeed, the SMPs are polymeric smart materials which have the remarkable ability to recover their primary shape from a temporary one when submitted to an external stimulus.

The present study deals with the synthesis and the thermo-mechanical characterization of a thermally-actuated SMP. The polymer considered hereafter is a chemically cross-linked thermoset. It is synthesized via photo polymerization (UV curing) of the monomer *tert*-butyl acrylate (tBA) with the crosslinking agent poly(ethylene glycol) dimethacrylate (PEGDMA) and the photoinitiator 2,2-dimethoxy-2-phenylacetophenone (DMPA).

A mechanical characterization has been performed using three kinds of tests: quasi-static tensile tests, tensile dynamic mechanical analysis (DMA) and modal tests. The Young's modulus and the Poisson ratio are determined at ambient temperature using the first technique. The DMA is used to determine the evolution of viscoelastic properties as a function of the temperature and the frequency under harmonic loading. The modal analysis is employed to identify the viscoelastic properties of the material at higher frequency. A comparison of the results obtained by these three experimental methods highlights their complementarity.

1 INTRODUCTION

Shape memory polymers (SMPs) belong to the class of smart materials. These materials have found growing interest throughout the last few years. Indeed, in some aspects, SMPs are more efficient than the well-known metallic shape memory alloy (SMA's). SMPs particularly offer recoverable strain that can reach 400% (to be compared to 8% for SMAs), light weight, easy manufacturing and cheapness compared to SMA [1]. They can be used in a large variety of applications, e.g. actuators, electromechanical systems, clothing manufacturing, morphing and deployable space applications, control of structures, self-healing, biomedical devices and so on [2, 3]. The SMPs have the ability of changing their shape in response to an

* pauline.butaud@femto-st.fr

external stimulus [4], most typically thermal activation. When the SMP is heated above the glass transition temperature T_g , it is soft and rubbery and it is easy to change its shape. If the SMP is subsequently cooled below T_g , it retains the given shape (shape fixing characteristic). When heated again above T_g , the material autonomously returns to its original permanent shape [5]. The shape-memory effect is in principle a behavior inherent to all polymers. However, polymers that exhibit truly exploitable shape-memory effect must demonstrate a sharp transition temperature and a rubbery plateau, along with relatively large strain capacity without local material damage [6]. The memory effect of SMP is quite depending on the level of external constraint. For example if the stiffness of the constraining material is equal to the stiffness of the shape memory polymer in the rubbery state, the polymer will only recover half of its total strain [7].

The increasing use of SMP for quasi-static and dynamic applications, under various temperature ranges, has made necessary the characterization of these materials over wide frequency bands [8]. Three kinds of tests have been performed in this study. First, quasi-static tensile test are used at ambient temperature and at a controlled loading rate permit to identify the Young's modulus. Then, a dynamic mechanical analysis (DMA) is used to determine the evolution of viscoelastic properties as a function of the temperature and loading frequency. Finally, a modal analysis has been performed to reach higher loading frequencies. In this last technique, a finite element model is employed to identify the viscoelastic properties of the material from the dynamic measurements. The main purpose of this work is to check the validity of the time-temperature equivalence [9] obtained from the DMA measurements, and more exactly to check the capacity of DMA on a restricted frequency range and at various temperature levels to predict accurately the viscoelastic properties on a wider frequency range. The predicted viscoelastic properties are compared to the measurements collected using quasi-static and modal test. This is an important query considering that measurement combining several experimental methods is particularly time-consuming.

2 MATERIALS AND EXPERIMENTAL METHODS

2.1 Material and specimen preparation

As a representative thermally-actuated shape-memory polymer, a chemically-crosslinked thermoset polymer recently studied by Yakacki et al. [10] and Srivastava et al [11] is chosen. Following the procedure described by these authors, the SMP is synthesized by manually mixing 95 wt% of the monomer *tert*-butyl acrylate (tBA) with 5 wt% of the crosslinking agent poly(ethylene glycol) dimethacrylate (PEGDMA) (with typical molecular weight $M_n = 550$ g/mol). The photoinitiator, 2,2-dimethoxy-2-phenylacetophenone (DMPA), is added to the solution at a concentration of 0.5 wt% of the total weight. The liquid mixture is then injected between two glass slides separated by a 3 mm spacer. The polymerization is initiated by exposing the solution to UV light during 10 minutes and achieved by heating the polymer at 90°C for 1 hour.

One of the obtained plates, measuring 200 × 150 mm, was machined with a CNC machine. Dog-bone shaped specimens were produced from the polymer plate for quasi-static tensile tests. The gauge length is 35 mm, and the rectangular cross section is 2.9 × 6.8 mm. In the same plate, samples for DMA testing were cut to 110 × 4 × 2.9 mm. Another plate was produced with the exact same protocol for the modal analysis measurements.

2.2 Mechanical tests

2.2.1 Quasi-static tests

The quasi-static tensile test have been performed using a universal commercial testing machine (Instron 6025) with a capacity of ± 100 kN. The specimen, clamped using wedge action grips, was subjected to a displacement control feedback at a rate of 1 mm/min. The test was performed at ambient temperature 21°C ($\pm 1^\circ\text{C}$). The engineering longitudinal strain was measured by a laser extensometer (EIR LE05) with a displacement accuracy of approximately $1\ \mu\text{m}$. The gauge part of the specimen for the strain measurement is 33 mm in length. The longitudinal Young's modulus was determined by the slope of the stress-strain curve at 0.1% of engineering strain (tangent modulus technique).

2.2.2 Dynamic mechanical analysis

Viscoelastic properties (storage modulus, loss modulus and loss factor) are measured using a Bose Electroforce 3200 apparatus every 5°C in isothermal conditions. Temperature varies between -28°C and 30°C , the frequency of the solicitation from 0.1 Hz to 10 Hz. The temperature is stabilised during 2 minutes before measurements to ensure a homogeneous temperature inside the specimen. The heating rate is about $0.1^\circ\text{C}/\text{sec}$ between each plateau temperature. The temperature is measured using a thermocouple positioned in a reference sample put in the heating chamber close to the tested specimen.

The compliance of the test set-up was taken into account for the determination of the viscoelastic properties.

A sinusoidal tensile load was applied on the sample with a mean amplitude of 2 N and a peak-to-peak amplitude of 3 N, in order to test the specimen in the linear viscoelastic range. Loading-unloading tests were also made on this equipment, at temperature below and above the glass transition. A tensile load from 0.1 N to 5 N was applied on the sample with a constant rate of 0.2 N/s, between -15°C and 30°C every 15°C . After the glass transition, between 70°C and 90°C (every 10°C), a tensile ramp of 0.05 N to 0.15 N was applied on the sample at a rate of 0.005 N/s. At high temperature, a more sensitive load cell was used considering the high decrease in rigidity of the tBA/PEGDMA and to ensure accurate measurements. It should be emphasized that at this temperature level the specimen stiffness is only of $0.1\ \text{N}\cdot\text{mm}^{-1}$.

2.2.3 Modal analysis

The studied structure is a tBA/PEGDMA rectangular plate with dimensions $157.7 \times 45.5 \times 3.1\ \text{mm}$ ($\pm 0.1\ \text{mm}$). The plate is suspended in order to realize free-free conditions. Contactless actuators and sensors are used. The external force is applied thanks to a voice-coil actuator with a permanent magnet glued in a corner of the plate. This assembly is placed in a thermal chamber with a temperature control between 22 and 36°C every 7°C ($\pm 2^\circ\text{C}$). A broadband random excitation is applied between 150 and 4000 Hz. The plate response is measured by using a laser vibrometer (Polytec OFV-505) successively focused on 28 reflecting stickers spread on the plate. The modal frequencies, the modal damping and the mode shapes are then identified by using Modan© (homemade modal analysis software). At the same time, a finite element model is established on PatranTM2012 under the hypothesis that the material is homogeneous and isotropic, with a Poisson's ratio $\nu = 0.37$ (determined from quasi-static tests), a mass density $\rho = 1004\ \text{kg}/\text{m}^3$ (determined by measuring the plate's mass and volume) and a presumed Young's modulus $E = 2000\ \text{MPa}$. The magnet is included in the numerical model ($E = 210\ 000\ \text{MPa}$, $\nu = 0.33$, $\rho = 7460\ \text{kg}/\text{m}^3$). Finally a model-test correlation is performed on AESOP software and a model updating procedure is conducted to obtain the mechanicals parameters of the tBA/PEGDMA at the modal frequencies.

2.2.4 Infrared thermography

Thermal field was monitored by infrared thermography using a CEDip Jade III MWIR camera. It provides 320×240 pixels images. The acquisition frequency is set to 25 Hz and the integration time is $430\ \mu\text{s}$. The

measuring range was 5-90°C. The measurements were performed during quasi-static tests and DMA to visualize the possible overheating in the sample.

2.2.5 Kinematic fields measurement

An optical camera (Ueye 1Mpixel 8bit) was used to assess the displacements fields in the gauge part of the specimen using digital image correlation (DIC). The camera was equipped of a telecentric lens (0.20x Techspec Silver series telecentric lens - 63073 - Edmund Optics) that prevents measurements from optical distortions. It also ensures a large depth of field (of approximately 6 mm) which guarantees the sharpness of images even in case of necking. Image acquisition was triggered using a Labview application at a frequency of 1 frame per sec. DIC was performed with a free home-made global correlation code, implemented in Octave and described by Maynadier et al. [12]. Quadratic elements were chosen for meshing the area of interest. The strain fields were computed from the displacement fields by pixel-wise difference gradient.

3 RESULTS

3.1 Quasi-static characterization

Figure 1 shows the stress-strain curve obtained from the quasi-static test. The apparent Young's modulus is approximately 1500 MPa, the ultimate stress (32 MPa) is reached at a strain of 1.8% and the elongation at rupture is about 60 %.

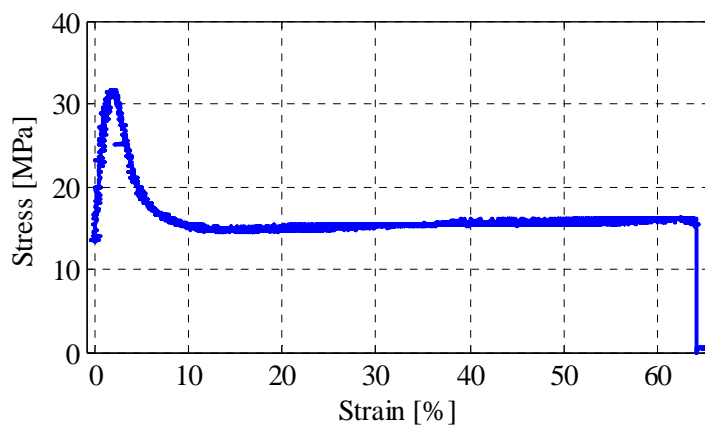


Figure 1. Stress – strain curves in tensile test at 1 mm/s, for tBA/PEGDMA, at ambient temperature

Infrared thermography was used for visualization of the temperature field at the surface of the specimen during this test. As shown in figure 2, the thermo-mechanical behavior of the tBA/PEGDMA in quasi-static is quite similar to the classical polymer's behavior: there is a cooling during the elastic phase, then a warming during the viscoelastic phase. Heat release is localized first in the necking zone and then heat propagates along the sample. Finally, rupture occurs with high heat release localized in a very sharp area around the crack tip.

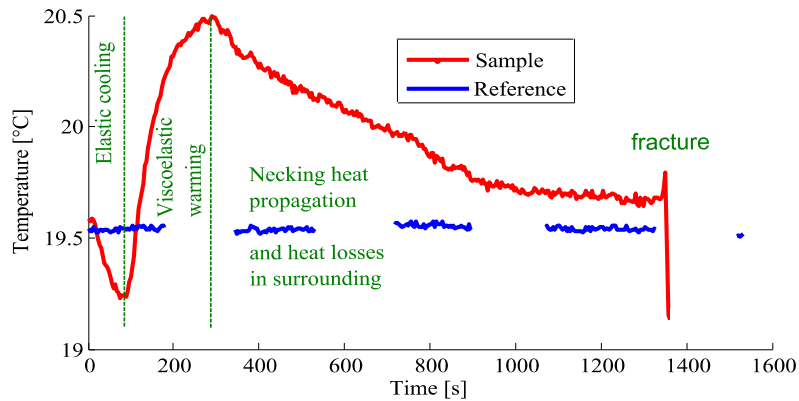


Figure 2. Temperature variation on the centerline of the sample compare to the ambient temperature at 1 mm/s

The Poisson's ratio was determined using the strain fields determined using DIC. The value is approximately 0.37 (Figure 3).

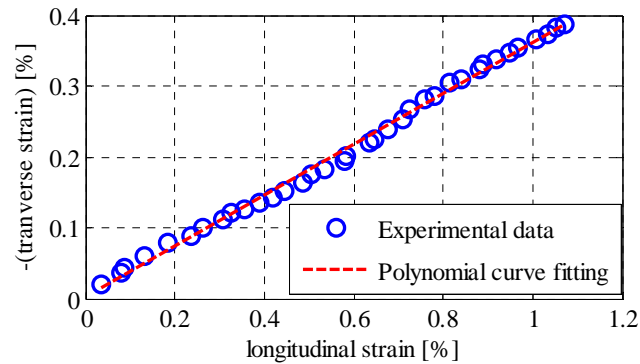


Figure 3. Identification of the Poisson's ratio around 0.37 at 1 mm/s

Figure 4 shows the high influence of temperature on the Young's modulus. Its value is almost constant, around 2060 MPa from -20°C to 40°C and also constant but 2500 times lower (0.8 MPa) above 60°C. This abrupt change in the elastic modulus reveals a phase transition between 40°C and 60°C.

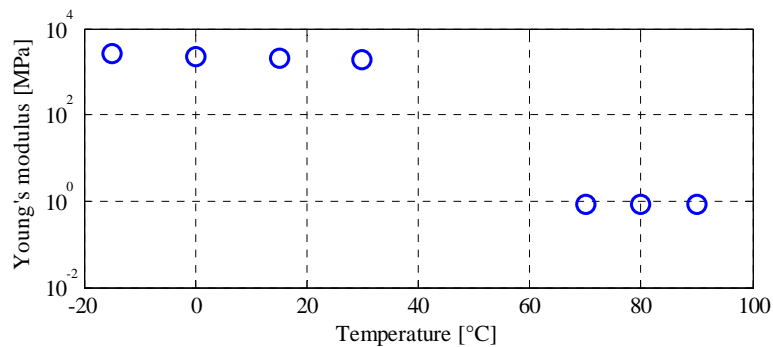


Figure 4. Stress – strain curves in tensile test at several temperature

The temperature variation registered by infrared thermography was not significant during this kind of tests; the variation level is lower than the noise level. The hypothesis of isothermal test is verified, there is not self-heating of the sample under mechanical solicitation.

3.2 Dynamic mechanical analysis

The results of the DMA tests are shown in Figure 5. The storage modulus decreases with the temperature and increases with the frequency. On the contrary, the loss factor increases with the temperature and decreases with the frequency. These trends are coherent with the classical behavior of a polymer without measurements on the transition area. Moreover the values of E' and $\tan \delta$ at 1 Hz are consistent with the results on the tBA/PEGDMA of Ortega et al. [13].

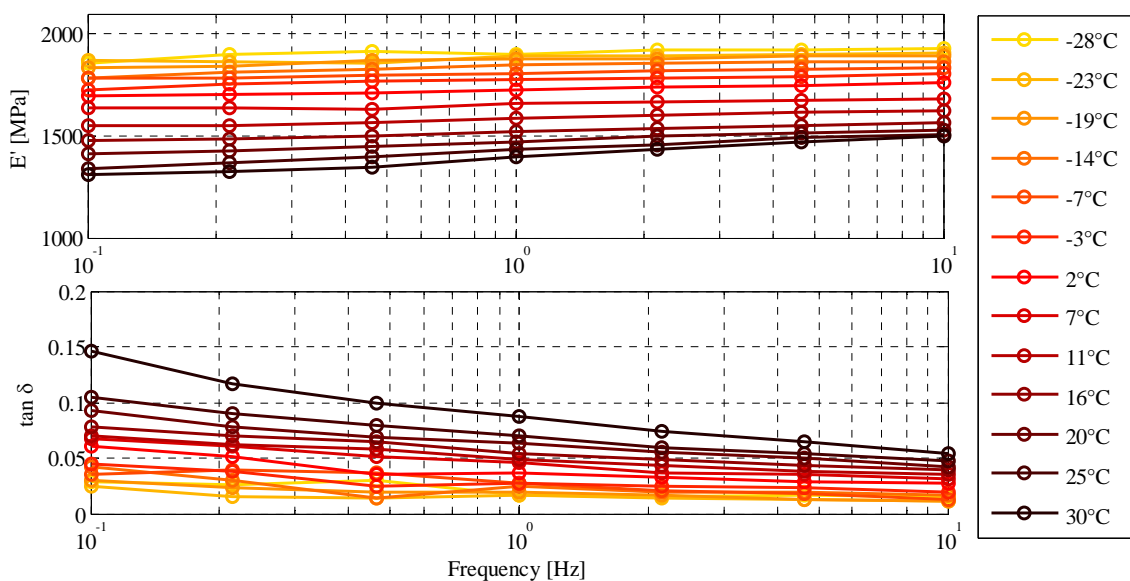


Figure 5. E' and $\tan \delta$ according to the frequency and for several temperatures

Curves of E' vs. frequency at one temperature can be shifted to overlap with adjacent curves (Figure 5). The time-temperature superposition shift factors a used for E' must be the same for $\tan \delta$ to get time-temperature equivalence [14]. In our case, the shift factors a are obtained through an optimization procedure (classical least square method) and are equivalent for both E' and $\tan \delta$, therefore the time-temperature equivalence is validated in a specified temperature and frequency ranges for the tBA/PEGDMA. The master curves of the storage modulus and $\tan \delta$ are given in Figure 6.

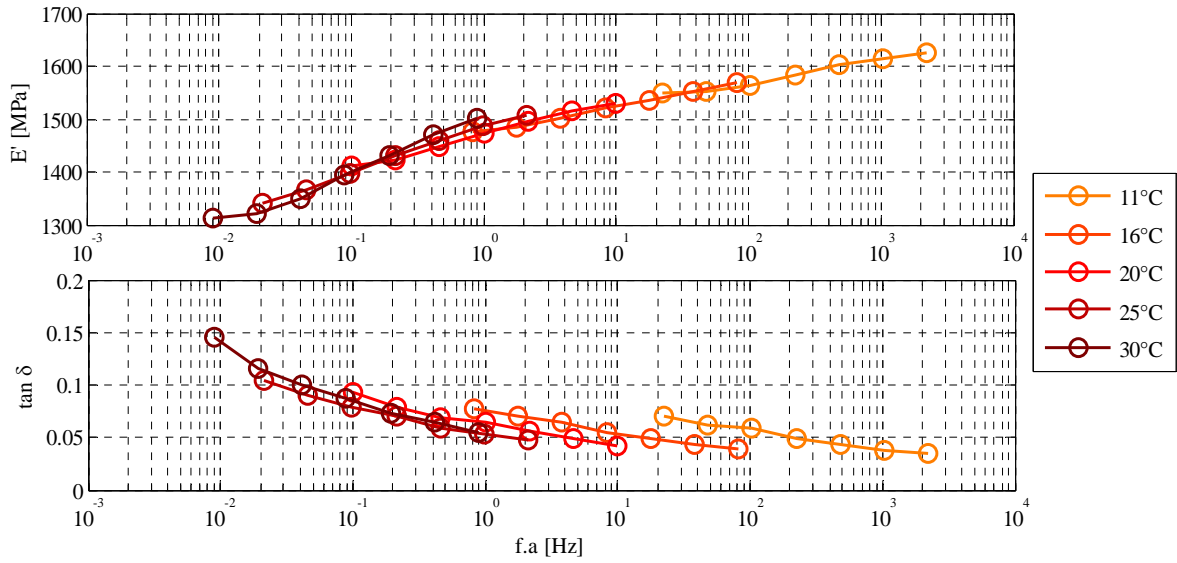


Figure 6. Master curves of E' and $\tan \delta$ according to the reduced frequency with a reference temperature of 20°C

3.3 Modal analysis

Depending on the temperature, 11 to 13 modes are identified after the model-test correlation (Figure 7).

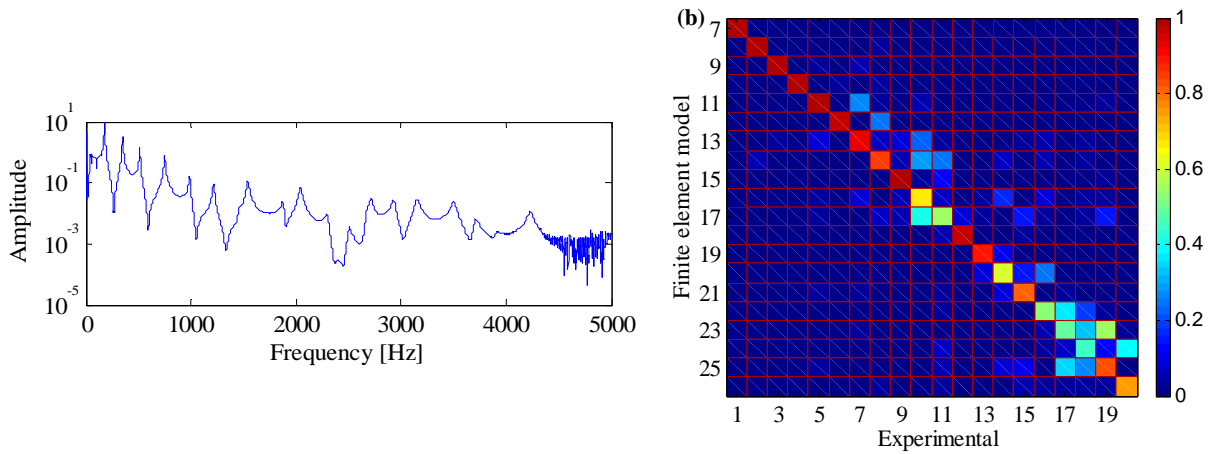


Figure 7. (a) FRF and (b) MAC Matrix for 22°C experimental data

Just as for DMA, the obtained Young's modulus and $\tan \delta$ of the tBA/PEGDMA depend on the temperature and the frequency as shown in Figure 8.

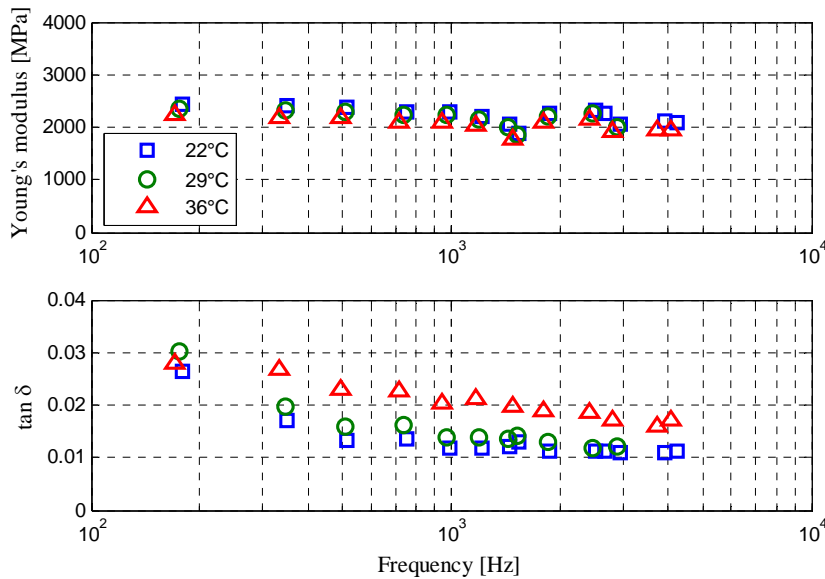


Figure 8. E' and $\tan \delta$ according to the frequency and for several temperatures

As expected, the loss factor increases with the temperature and decreases with the frequency. Concerning the storage modulus, it decreases as planned with the temperature but its variation with the frequency is unusual, as it decreases too. This trend is not well understood yet, even if some hypotheses are considered. For example, the Poisson's ratio used in the finite element model was determined in quasi-static regime whereas it could fluctuate with the frequency like the storage modulus. Other hypotheses like the isotropic character of the material are currently under investigation.

4 DISCUSSION

This study intends to compare the master curves obtained with the DMA and the results collected by the modal analysis and the quasi-static tests. Based on the time-temperature equivalence determined by DMA, the storage modulus predicted by this equivalence should be equal with the quasi-static and modal modulus, likewise for the loss factor. The DMA master curves and the results of quasi-static tests and modal analysis in temperature beforehand translated thanks to the shift factor are plotted on a same graphic (Figure 9). To define the frequency of the quasi-static test, the loading-unloading test period was taken in account, thus the frequency of this test at low temperature is 0.02 Hz.

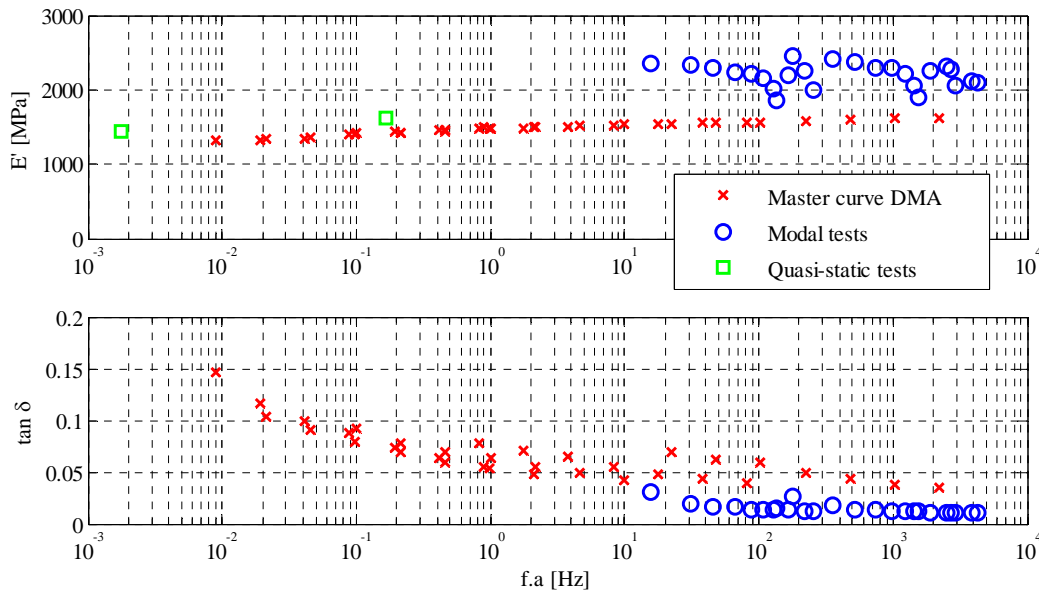


Figure 9. Comparison of experimental methods on E' and $\tan \delta$

The order of magnitude of E' at low frequency is respected. The time-temperature equivalence data are consistent with the quasi-static results. At high frequency, there is a gap of about 50 % between the storage modulus prediction and the modal results. This is not observed for the loss factor, for which the comparison is quite conclusive.

There are some options to explain this gap between the modal tests and the master curve. First of all, the hypothesis of isothermal test could be unverified i.e. the sample could undergoes self-heating under mechanical solicitation. This possibility was eliminated for DMA tests with infrared thermography but not for the modal analysis. Secondly, as it was mentioned previously, the Poisson's ratio could be not correctly defined in the finite element model. Finally, the most important distinction between modal analysis and the two others experimental methods is the kind of solicitations. Indeed, whether for quasi-static or DMA, the test is in tensile on a beam sample, contrary to the modal analysis for which the test is in bending on a plate and for smaller strain amplitude. It therefore appears necessary to study the behavior of the tBA/PEGDMA in tensile and compression, and check whether a distinction. Lastly, a post-treatment is required for the modal data thanks to a finite element model, contrary to DMA and quasi-static data which are used unaltered.

5 CONCLUSION

The objective of this study was to highlight the time-temperature equivalence by comparing three experimental methods allowing the identification of the storage modulus over frequency and temperature. This equivalence has been checked on a sample tested with the DMA. Quasi-static tests and modal analysis have been carried out to explore a wider frequency band. Even though the results are rather consistent, the time-temperature equivalence is not yet established. Further investigations are needed to clarify the tBA/PEGDMA behavior. The correlation between quasi-static, DMA and modal analysis remains to be carried out.

References

1. Pretsch Thorsten, "Review on the functional determinants and durability of shape memory polymers", *Polymers*, Molecular Diversity Preservation International, 2010, Vol. 2, pp. 120-158
2. Behl, M. and Lendlein, A., "Shape-memory polymers", *Materials Today*, 2007, Vol. 10, pp. 20-28
3. Dietsch, B. and Tong, T., "A review-: Features and benefits of shape memory polymers (SMPs)", *Journal of advanced materials*, 2007, Vol.39, pp. 3-12
4. Ratna D. and Karger-Kocsis J., "Recent advances in shape memory polymers and composites: a review", *Journal of Materials Science*, 2008, Vol. 43, pp. 254-269
5. S.A. Wilson, R.P.J. Jourdain, Q. Zhang, R.A. Dorey, C.R. Bowen, M. Willander, Q.U. Wahab, S.M. Al-hilli, O. Nur, E. Quandt, et al., "New materials for micro-scale sensors and actuators: An engineering review", *Materials Science and Engineering: R: Reports*, 2007, Vol. 56, pp. 1-129.
6. B. Sillion, "Shape memory polymers", *Acta Chim*, 2002, Vol. 3, pp. 182-188.
7. Liu, Yiping and Gall, Ken and Dunn, Martin L and Greenberg, Alan R and Diani, Julie, "Thermomechanics of shape memory polymers: uniaxial experiments and constitutive modeling", *International Journal of Plasticity*, 2006, Vol. 22, pp. 279-313.
8. A. Lendlein and S. Kelch, "Shape-memory polymers", *Angewandte Chemie International Edition*, 2002, Vol. 41, pp. 2034-2057.
9. N. Okubo, "Preparation of Master Curves by Dynamic Viscoelastic Measurements", *SII NanoTechnology Inc.*, 1990, Vol. 6.
10. Yakacki, Christopher Michael and Shandas, Robin and Lanning, Craig and Rech, Bryan and Eckstein, Alex and Gall, Ken, "Unconstrained recovery characterization of shape-memory polymer networks for cardiovascular applications", *Biomaterials*, 2007, Vol. 28, pp. 2255-2263.
11. Srivastava, Vikas and Chester, Shawn A and Anand, Lallit, "Thermally actuated shape-memory polymers: Experiments, theory, and numerical simulations", *Journal of the Mechanics and Physics of Solids*, 2010, Vol. 58, pp. 1100-1124.
12. A. Maynadier, S. Carbillet, V. Placet, F. Amiot, A. Seror, A. Longuet, C. Mary, "Fatigue behaviour of D.A. INCONEL 718 alloy under tension-torsion loading". In *PhotoMechanics*, Montpellier, 2013
13. Ortega, Alicia M and Kasprzak, Scott E and Yakacki, Christopher M and Diani, Julie and Greenberg, Alan R and Gall, Ken, "Structure-property relationships in photopolymerizable polymer networks: Effect of composition on the crosslinked structure and resulting thermomechanical properties of a (meth) acrylate-based system", *Journal of Applied Polymer Science*, 2008, Vol. 110, pp. 1559-1572.
14. Dealy, John and Plazek, Don, "Time-temperature superposition—a user's guide", *Rheol. Bull*, 2009, Vol. 78, pp. 16-31